The influence of curvature on FLC's of mild steel, (A)HSS and aluminium

E.H. Atzema[1], E. Fictorie[2], A.H. van den Boogaard[2] & J.M.M. Droog[1]
[1]Corus RD&T, PO Box 10000, NL-1970 CA IJmuiden
[2]University of Twente, PO Box 217, NL-7500 AE Enschede
eisso.atzema@corusgroup.com

Abstract: In literature the influence of curvature on formability has been reported. This paper shows results for four materials when an FLC is measured with increasing curvature. It shows the FLC increases for sharper curvature most notably with 20 [mm] tool diameter. The increase is negligible on the left hand side, moderate on the right hand side and large on the plane strain axis. It is thought that contact pressure plays a role here and preliminary simulations indicate that this is quite possible.
Keywords: FLC, AHSS, Aluminium, curvature

1. INTRODUCTION

The authors observed that the commonly used FLC is too often conservative in highly curved areas. The formed product shows no sign of failure in these conditions, even though the strains exceed the FLC, something also reported by others [Till et al, 2008]. The influence of curvature on the FLC has been reported less, notwithstanding the efforts on stretch bendability, see for instance [Geoffroy et al, 2007] and much earlier [Charpentier 1974]. These papers report some indicative FLC points, but a full FLC has never been measured. Since curvature seems to have more impact on AHSS, and these steels are increasing in importance, it becomes paramount for the steel industry to characterize and understand the effect in order to optimize the use of these materials.

This paper reports the influence of curvature on the entire FLC for steels DC06, H340LAD+Z and HCT600X+Z as well as AA 5051 aluminium. The FLC was established by measuring the strains from samples subjected to the Nakazima test. The ISO standard 12004-2 recommends a Ø100 mm hemispherical punch to deform test samples of different widths. In this work the influence of curvature was investigated by using Nakazima experiments with punch diameters of 20, 50 and 75 [mm], referred to in this paper as FLC20, etc. A support of a PUR disk with Teflon sheets and Vaseline spray was inserted between the punch and the sample to obtain sample failure on the top of the sample as recommended in the ISO standard. The sample dimensions as well as the PUR disk were scaled with the punch diameter.

The first tests made it clear that the downscaled support-system for the FLC20 setup failed through perforation caused by high contact pressure. A slightly adapted support-system did sustain the applied forces. The obtained FLC20, FLC50 and FLC75

were compared to the standard FLC100. The DC06 showed only slightly higher values in FLC for the 20 [mm] punch. The aluminium sheet and H340LAD+Z both showed a slight improvement with the 50 [mm] punch and a major improvement with the 20 [mm] punch. Finally, the FLC20 for the HCT600X+Z showed considerably higher values than FLC100 and even the FLC50 was perceptibly higher.

The strongest effect was seen in the plane-strain region and only moderate effects were seen in uni-axial and bi-axial regions.

A first attempt at FE modeling was made to obtain the most influential factors, but this remains qualitative. Further research will be required to reveal the effect of different thicknesses and refine the model to return a quantitative prediction of the effect.

Results for DC06 and AA5051 have been reported earlier in [Fictorie et al, 2010]

2. EXPERIMENTAL SETUP

2.1. Necking limit

Although an FLC on fracture can be constructed, the necking FLC is most widely used, since necking is not usually acceptable. The FLC is defined as the strain combinations for which localized necking starts i.e. for which the sheet becomes plastically unstable. After localized necking, the part will eventually fracture.

The necking analysis of a tensile test is generally based on the Considère criterion: $d\sigma/d\varepsilon=\sigma$. This stems from the consideration that if the force that can be exerted on a tensile test sample drops, a part of it will neck and the rest will unload. The force drops after a maximum is reached or mathematically: $dF=0$. Necking in an FLC is different in that a diffuse neck (neck over the width) cannot develop since the width of the sheet is not free to contract such as it is in a tensile test. In fact, the FLC represents localised necking, i.e. a neck over the thickness, of the material. But a similar analysis on maximum force can be still done. In this analysis one assumes constant strains over the thickness to come from a force maximum to a strain based necking criterion.

In realising this, we know that an FLC applies only to flat sheets, or approximately to slightly curved ones. The recommendation of the last working group on FLC's to use at least 100 [mm] diameter punch for a Nakazima test must be viewed from this perspective.

Pure bending does not involve a normal force and therefore even when the strain on the outer (more deformed) fibre is above the FLC this still does not cause necking (i.e. instability). In pure bending the inner fibres are compressing, for the inner fibres to stretch a normal force needs to be added to the bending moment. In a situation of combined stretching and bending [Vallellano et al, 2008] assumes overall sheet necking will occur once the inner fibres are strained beyond the FLC, similar to [Tharrett et al 2003]. This has become known as the "concave side rule".

In a similar manner to the FLC one can obtain the limit strains in bending. Usually no necking occurs but cracks show up at the surface. These can be plotted in an FLD like diagram as well, see [Schleich et al, 2009].

If stretch is added to bending, necking is more likely to occur. But it is not a priori clear that a linear transition from FLC to bending strain limit exists as for instance proposed by [Schleich et al, 2009]. In fact a rigorous analysis on the maximum normal force under simultaneous bending is needed; something akin to what [Kruijf et al, 2009] did for simple stretch-bending. Since this needs material modelling and some kinematic assumptions it was decided to leave this sort of analysis to a later stage and first establish the order of magnitude of the effect by experiments.

2.2. Standard FLC setup

Corus routinely performs FLC determination by Nakazima testing. Up until a few years ago, a 75 [mm] diameter hemispherical punch was used, but nowadays a hemispherical punch of 100 [mm] diameter is used. For the 100 [mm] punch a die inner diameter of 106 [mm] with a die radius 8.6 [mm] is used. Circular blanks are cut from the material in a diameter of 200 [mm] and from these the sides are subsequently cut-out to produce a dogbone shape. A stack of these in different width can be seen in **Figure 1**.

Figure 1; Stack of dogbone FLC samples for 100[mm] hemispherical punch.

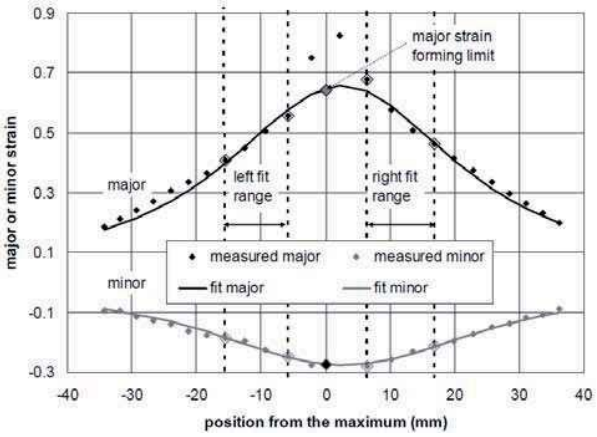

Figure 2; Schematic evaluation strain data.

The lubrication system from the sheet downwards to the punch consists of a PUR pad, then Vaseline spray, a Teflon foil, more Vaseline spray and another Teflon foil. The PUR pad is Erlan of ∅ 80 [mm], 4 [mm] thick and the Teflon foil is Eriflon 0.05 [mm] thick ∅ 100 [mm]. The punch speed during this test is 40 mm/min.

The evaluation of data was done according to ISO 12004-2 with an in-house code in MS-Excel. A schematic explanation is given in **Figure 2** of how we arrive at an FLC value from a measured strain distribution. At both sides of the two largest values a fit range is fixed (see ISO 12004-2). The thickness strain is calculated by volume invariance. Then an inverse parabola is fitted through the major strain distribution as well as the thickness strain distribution. An inverse parabola on the minor strain (which can be zero) is not robust. From these fits, the minor strain is recalculated from volume invariance. The FLC value is then sampled on the parabola in the mid point between the two largest values. For each FLC sample, five strain sections are evaluated.

2.3. Test setup

In addition to the above mentioned sizes, a 50 [mm] and 20 [mm] diameter hemispherical punch was available. These tools were used to extend the FLC determination by Nakazima method to four different punch sizes.

Corus employs a partially and fully serrated blankholder in the FLC100 and FLC75 to provide sufficient clamping. These serrated tools are specific for FLC and were not available for the 50 [mm] and 20 [mm] punches. Consequently, the dies and blankholders had to be adapted by machining serrations onto one surface of the toolset. Initially the dies were serrated, see **Figure 4**, starting next to the die radius and in a pattern concentric with the die opening. For the FLC50 this proved problematic and alternatively the blankholder was serrated straight and on a larger area, **Figure 3**. The tooling is therefore not scaled exactly but rather made to work properly. In section 3.1 it is shown this has no influence on the results.

2.4. Lubrication system

Between the punch and the test sample there are usually some additional layers of materials and lubricants, which is generally referred to as the *lubrication system* although this term is in fact misleading. Although the Teflon and Vaseline spray will indeed lubricate very well on the punch side, the PUR pad actually works because it sticks to the sheet and drives the material away from the top through friction as demonstrated by [Vegter et al, 2008].

In scaling the test, the PUR was also scaled in diameter and thickness from ∅ 80 [mm] and 4 [mm] thickness respectively. However, the FLC20 tests failed because the rubber was destroyed in the test, and we had to resort to 2 [mm] thick 16 [mm] diameter PUR. Underneath the PUR two Vaseline sprayed Teflon foils were always used. These were scaled in diameter but not in thickness as they were already very thin.

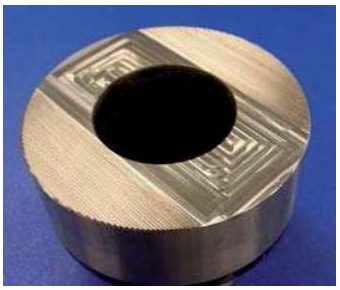

Figure 3; Partially serrated BH FLC50.

Figure 4; Partially serrated die FLC20.

2.5. Sample geometry

The sample geometry was again scaled as well as possible, but the specific cut-outs available for the FLC100 and FLC75 were simply not available for FLC50 and FLC20. Therefore from the range of available punches, one was chosen that represented the best compromise between narrowing needed to force the failure in the forming zone and a large enough area with parallel sides to ensure uniform strain distribution over the

width. Moreover the FLC20 samples became so small that it was impractical to blank them round and then apply the cut-out. These therefore remained rectangular.

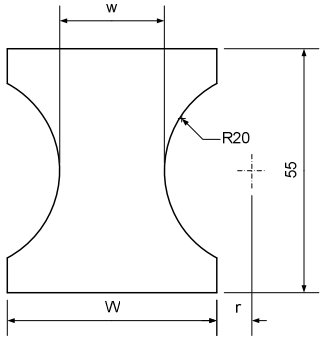

Figure 5; Sample geometry BH FLC20.

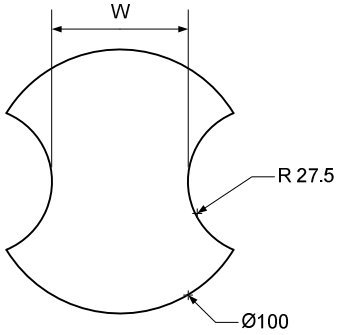

Figure 6; Sample geometry BH FLC50.

2.6. Materials tested

Four materials were tested and the choice was based on the amount of information already available of these materials in view of future modelling. The mechanical properties can be seen in **Table I**.

Table I; Mechanical properties of tested materials.

Material	R_m [MPa]	R_p [MPa]	t [mm]	A_{80} [%]	n [-]	r [-]
DC06	301	141	0.7	44.7	0.24	2.1
AA5051	189	90	1.0	20.4	0.24	0.7
H340LAD+Z	449	372	1.0	27.6	0.14	1.0
HCT600X+Z	635	391	1.4	21.1	0.15	1.0

3. RESULTS

The DC06 will be presented in somewhat greater detail to illustrate the method. The other materials, due to lack of space, will be presented concisely.

3.1. DC06

DC06 is a forming grade steel and can therefore reach high strain values before failure. This led to problems with the use of the partially serrated die in the initial FLC50 experiment, where samples were stretched very high. The serrated area appeared to be too small and therefore initially the solution was to use of a fully serrated die, after which the failure was obtained in the top.

As stated in section 2.3, these problems were permanently solved by a new partially serrated blankholder. In *Figure 7* the measured necking points are presented for the FLC50 experiments with a serrated die or with serrated blankholder. It can be seen that the results are reasonably reproducible. All results are in true strain.

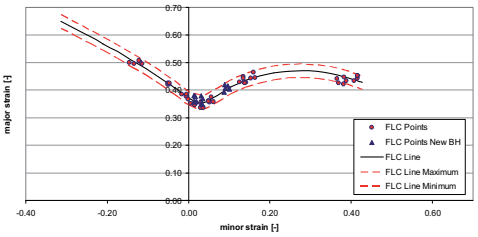

Figure 7; FLC50 points for DC06, including FLC points of samples tested with the serrated blank holder.

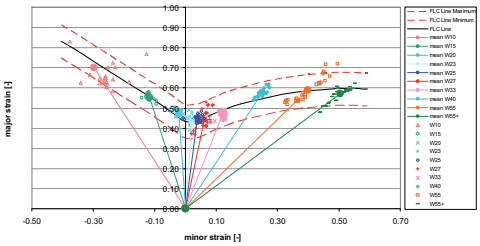

Figure 8; FLC20 points for DC06 all sections on all samples.

In *Figure 8* the measured necking points are presented for the FLC20 experiments. The experimental scatter is higher in this case, which should be kept in mind when comparing the results with the results for the other punch diameters.

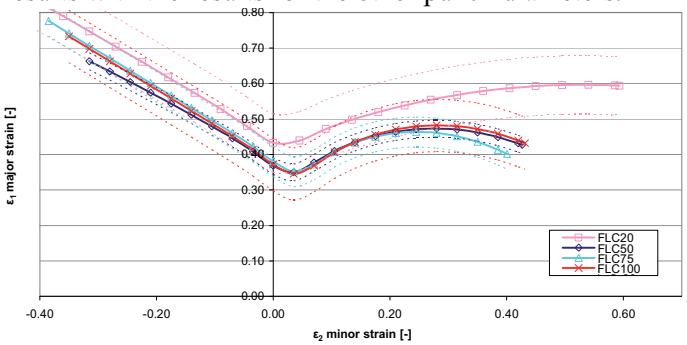

Figure 9; FLC comparison for DC06.

By comparing all FLC's (**Figure 9**), it can be seen that the curves of the FLC100, FLC75 and FLC50 are very close to each other. The FLC20 curve is also quite close to the other curves, but there is a slight difference. Incidentally, the points shown span the FLC curve and are not measured points. The dotted lines represent the 2σ variation to give an indication of the test noise. A rigorous analysis of the confidence interval was not made at this stage, so a statistical significance cannot be concluded.

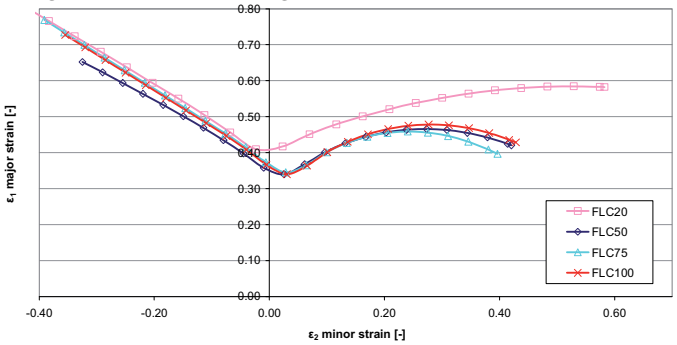

Figure 10; FLC comparison for DC06 after mid-plane.

After correcting the measured strains towards the mid-plane of the sheet (**Figure 10**), the FLC20 curve is at the same level as the other formability curves in the compressive region. In the right hand side of the FLC, there is an increase of formability obtained continuing until the biaxial point, of about 20% relative, i.e. a factor of 1.2.

For the other materials only this final figure, showing mid-plane strains, will be presented.

3.2. AA5051

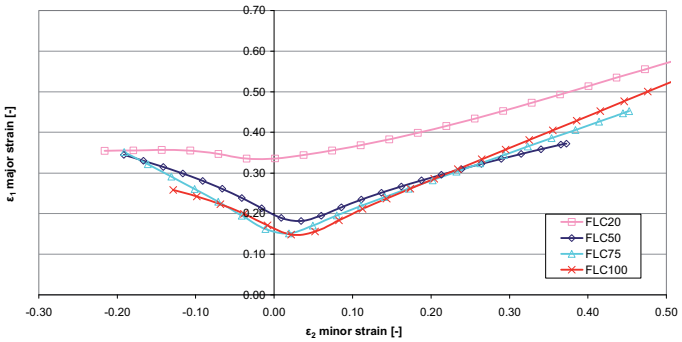

Figure 11; FLC comparison for AA5051 after mid-plane correction.

The aluminium AA5051 again shows a major increase in formability for the FLC20 over the others (**Figure 11**). But now some improvement in formability for the FLC50 is also apparent. The improvement is less towards the extremes most notably the left hand side of the FLC. In the plane strain region, an increase of a factor of 2.0 is seen for FLC20 relative to the FLC100. The formability increase obtained from the FLC50 experiment is only in the plane strain and compression region. The biaxial samples of the FLC50 were not truly equi-biaxial: minor strain was only 0.30, so for $\varepsilon_1 > 0.30$ it is not realistic to compare the results, since there the FLC curve is an extrapolated fit.

3.3. H340LAD+Z

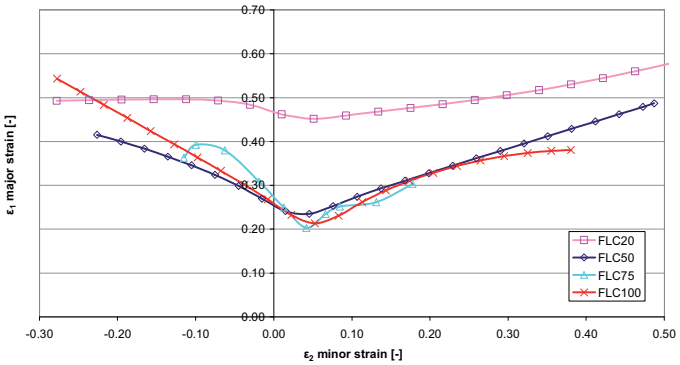

Figure 12; FLC comparison for H340LAD+Z after mid-plane correction.

Like for DC06 for this material FLC50, FLC75 and FLC100 are all similar. But again the FLC20 is markedly higher. And again on the plane strain axis the effect is largest, this time slightly less than a factor 2.0. It can also be seen that the FLC75 was a bit messy and in general the curves differ a bit in shape for FLC50, FLC75 and FLC100.

3.4. HCT600X+Z

As with the AA5051 a slight, maybe insignificant, increase can be seen for FLC50 with respect to FLC75 and FL100, which are virtually indistinguishable. The FLC20 once again shows a major increase. And also on this occasion the extreme left area of the FLC shows no improvement and the biaxial point only a moderate improvement. The major effect is seen around the plane strain axis, which now is a factor of around 2.3.

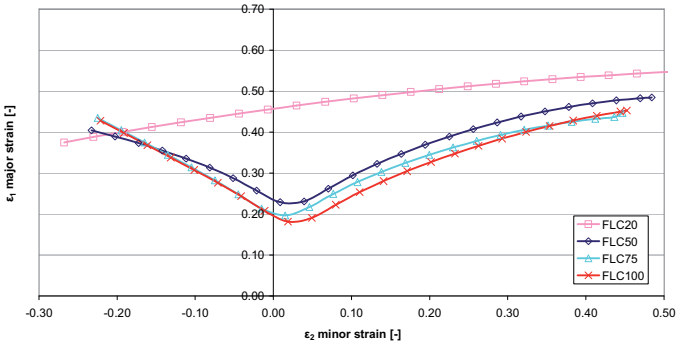

Figure 13; FLC comparison for HCT600X+Z after mid-plane correction.

4. DISCUSSION

A small, but still significant, difference in FLC was seen when going to 20 [mm] tooling for DC06. For AA5051 and H340LAD+Z the difference was larger and the difference was very large for HCT600X+Z. For the latter three materials the increasing trend was already seen in FLC50 as well. However, since the materials for this study were chosen based on available characterisation in view of future modelling a compromise was made: not all materials had the same thickness. So now the effect of grade and thickness are confounded. It does seem clear however there is a real effect and it increases either with thickness or grade, since the HCT600X+Z was the thickest as well as the strongest. Since FLC20 for all materials has a much larger difference with FLC50 than FLC50 with FLC 100 the effect seems strongly non-proportional with thickness to curvature ratio. This indicates the relatively small thickness difference could have large effects.

In spite of all efforts taken to reduce the error in the strain measurements, it cannot be excluded that some awkward effects occurred and affected the strain measurements. Although the grid was scaled with the punch size, the neck still has the same characteristic length, so is represented by more points which may influence the FLC calculation according to ISO 12004-2 and schematically depicted in **Figure 2**.

The strains are measured on the outside of the sheet. With mid-plane correction, the FLC20 curves decrease more than the FLC50 and FLC100 curves because of the small punch diameter. However, the decrease is far less than the improvement of the formability for all materials. Therefore the error which is made by measuring on the outside of the sheet is not seen to be the main effect for the formability improvement. By looking at the concave side strains this produces the same shift yet again as from **Figure 9** to **Figure 10** for thickness of 0.7 [mm] (and twice this for 1.4 [mm]) this still is obviously not enough to explain the effect.

The increased formability may also be influenced by the lubrication-system, which draws the material away from the top. Since the scaled lubrication-system for the FLC20 failed by perforation, the thickness of the used lubrication-system now is twice the scaled thickness. This may influence the strain distribution more than hypothesized beforehand. On the other hand the failure of the lubrication-system is a strong indication that contact pressures are relatively higher in smaller tooling.

5. MODELLING

A very crude first attempt was made at modelling the effect of curvature. It was hypothesised that the contact pressure plays a role, either by shifting equivalent stress thereby stabilising the necking or by suppressing damage. To quantify the influence of contact stress on plasticity and damage a model with through-thickness stress is needed as well as a damage model. This was deemed too complicated for a first attempt and a simple PAM-Stamp model was made from which a *qualitative* prediction was sought.

From the stresses calculated in the simulation the equivalent stress was obtained. Then the contact stress was added and equivalent stress recalculated. Now obviously this does not represent a true stress state since the stress is no longer on the yield locus. But it does give an indication in which direction the stress would change if through thickness pressure was modelled in the sheet.

In the simulation the stress gradient over thickness was very similar for both FLC20 W23 and FLC100 W120 and roughly inverse to FLC100 W120 after correction (**Figure 14** right), i.e. inner fibre has lowest equivalent stress. The difference in gradient over thickness between smaller FLC tooling (**Figure 14** left) and FLC100 (**Figure 14** right) is thus entirely due to effect of contact stress. Note the different vertical scale.

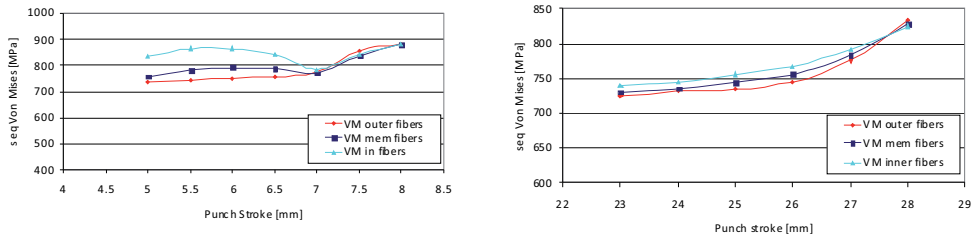

Figure 14; Equivalent stress with contact stress added FLC20 W23, FLC100 W120.

This provides a first indication that contact stress will play a role. The next step is to make a full model with the PUR pad modelled and including through-thickness stress in the sheet subjected to test.

6. CONCLUSIONS

- With smaller tooling an FLC could be reliably measured.
- For some materials, an increase in FLC is seen for 50 [mm] tooling and in all cases an effect is seen on 20 [mm] tooling.
- The effect is largest for HCT600X+Z which is the strongest but also the thickest, it cannot be concluded which of these is the major influence.
- The FLC goes up most markedly in the plane strain area. On both ends, left as well as right hand side, the increase is slight to insignificant

REFERENCES

[Till et al., 2008] E.T. Till, E. Berger, P. Larour, "On An Exceptional Forming Behaviour Aspect Of AHSS Sheets", *IDDRG 2008*, 16/18 June 2008, Olofström, Sweden

[Geoffroy et al., 2007] J-L. Geoffroy, J. Goncalves, X. Lemoine, Adequately Use FLC's For Simulation, *IDDRG 2007*, 21/23 May 2007, Györ, Hungary

[Charpentier 1974] P.L. Charpentier, "Influence Of Punch Stretching Curvature On The Stretching Limits Of Sheet Steel", *Metallurgical Transactions A. Physical Metallurgy 6A*, p.1665-1669, 1974

[Fictorie et al., 2010] E. Fictorie, A.H. van den Boogaard, E.H. Atzema, "Influence of curvature on the forming limit curve", *ESAform 2010*, 7/9 April 2010, Brescia, Italy.

[Vallellano et al., 2008] C. Vallellano, D. Morales and F.J. Garcia-Lomas: *"*On the study of the effect of bending in the formability of metal sheets", 1/5 September 2008, *Numisheet 2008* Interlaken Switzerland p.85-90, 2008.

[Tharrett et al., 2003] M.R. Tharrett and T.B. "Stoughton: Stretch-bend forming limits of 1008 AK steel", *SAE paper* 2003-01-1157, 2003.

[Schleich et al., 2009] R. Schleich, C. Held, M. Sindel, M. Liewald, „Investigation On The Effect Of Curvature And Sheet Thickness On Forming Limit Prediction For Aluminium Sheet Metal Alloys", *ESAform 2009*, Enschede, the Netherlands

[Kruijf et al., 2009] N.E. de Kruijf, R.H.J. Peerlings, M.G.D. Geers, "An Analysis Of Sheet Necking Under Combined Stretching And Bending", *ESAform 2009*, 27/29 April 2009, Enschede, the Netherlands,

[Vegter et al., 2008] H. Vegter, C.H.L.J. ten Horn, M. Abspoel, "Modelling of the forming limit curve by MK-Analysis and FE-Simulations", *Numisheet 2008*, 1/5 September 2008, Interlaken, Switzerland, pp187-192